

## Approximation theory

mathematical (noise free):

1. build  $H_\nu^{(0)}$ ,  $\nu = 0, 1, 2, \dots$
2.  $H_\nu^{(0)} = U\Sigma V^T$  singular value decomposition
3.  $\Sigma = \begin{pmatrix} \sigma_1 & & \\ & \ddots & \\ & & \sigma_\nu \end{pmatrix}$ ,  $\sigma_1 \geq \sigma_2 \geq \dots \geq \sigma_n > \sigma_{n+1} = \dots = \sigma_\nu = 0$
4. find  $\Omega_i, \phi_i, \alpha_i, i = 1, \dots, n$

## Approximation theory

numerical (with noise):

1. take  $\nu$  large enough so that noise is clearly separated from  $n$
2. solve  $H_\nu^{(1)} v_i = \lambda_i H_\nu^{(0)} v_i$ ,  $i = 1, \dots, \nu$ ,  $\lambda_i = \Omega_i$ ,  $i = 1, \dots, n$
3. find  $\phi_i$
4. solve  $\sum_{i=1}^n \alpha_i \exp(\phi_i x_j) = f_j$ ,  $0 \leq j \leq 2\nu - 1$

### Example: noise

$$\begin{aligned} \phi_1 &= 0, & \alpha_1 &= 1, \\ \phi_2 &= -0.2 + 39.5i, & \alpha_2 &= 2, \\ \phi_3 &= -0.5 + 40i, & \alpha_3 &= 4, \\ \phi_4 &= -1, & \alpha_4 &= 8, \end{aligned}$$

$$x_s = s \frac{2\pi}{100}, \quad M = 100$$

$$\|\varepsilon(z)\|_\infty = 10^{-2}, \quad \text{uniform random noise}$$

### Example: noise

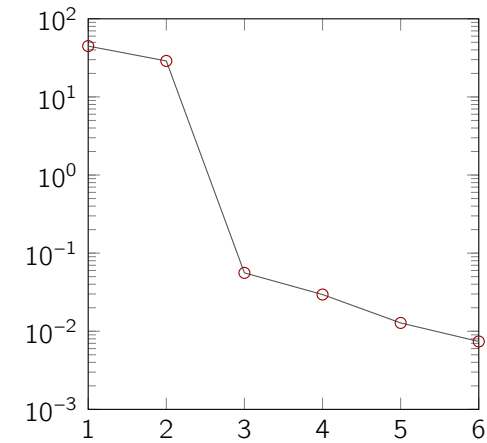


Figure: Singular values  $H_\nu^{(0)}$  with  $n = 4, \nu = 6$

### Example: noise

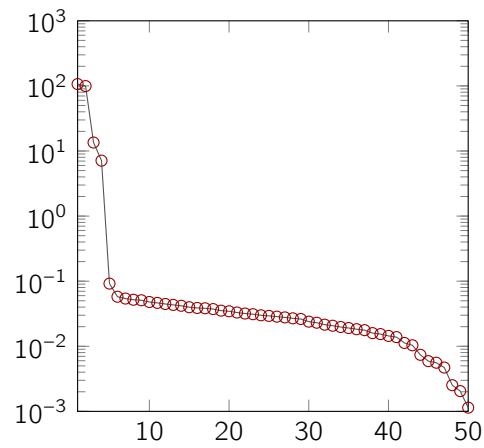


Figure: Singular values  $H_\nu^{(0)}$  with  $n = 4, \nu = 50$

### Exercise: approximation

$$\begin{aligned} \phi_1 &= 1.5i, & \alpha_1 &= 10^{-3}, \\ \phi_2 &= 12.7i, & \alpha_2 &= 2, & x_s &= s \frac{2\pi}{100}, \\ \phi_3 &= -0.1 + 40i, & \alpha_3 &= 4, & M &= 100 \\ \phi_4 &= -0.3 + 25.2i, & \alpha_4 &= 8, \end{aligned}$$

$$\|\varepsilon(z)\|_\infty = 2 \times 10^{-3}, \quad \text{uniform random noise}$$

```

format long;

phi = [1.5*1i, 12.7*1i, -0.1+40*1i, -0.3+25.2*1i];
alpha = [10^(-3), 2, 4, 8];

eps = 2*10^(-3);

M = 100;

plot_signal

pause

plot_fft

pause

% synthesized input data with added noise
N = input('Enter the dimension for SVD: ');
% (10, 6, 3), (100, 100, 4)

randn('seed',0);

omega = 2*pi/M*(0:2*N-1);
f = syn_exp(alpha, phi, omega);

v = randn(size(f))+randn(size(f))*1i;
vv = v/norm(v,Inf);
f = f + eps*vv;

% form Hankel matrices H0 and H1 from y sequence
[H0,H1] = mat_ge(f);

plot_svd

pause

% reconstruct the parameters via generalized eigenvalues
n = input('Size of the model: ');

```

```

% compute the generalized eigenvalues and form the Vandermonde system
E = eig(H1(1:n,1:n),H0(1:n,1:n));
V = rot90(vander(E));

% amplitudes
A = V\f(1:n).';

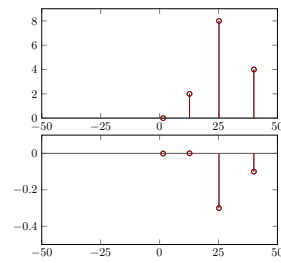
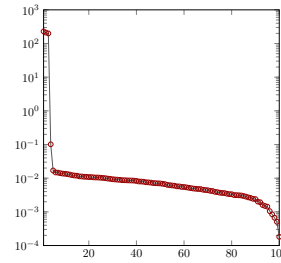
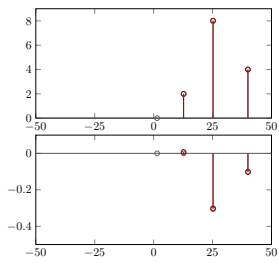
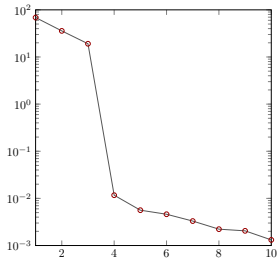
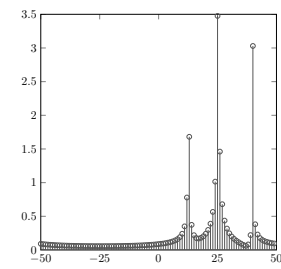
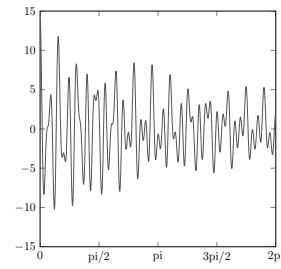
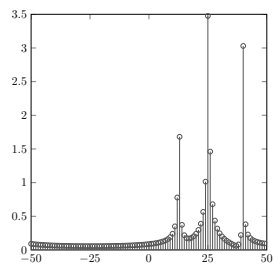
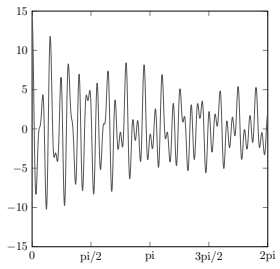
% frequencies and damping factors
alpha_rec = A;
phi_rec = log(E)*M/(2*pi);

pause

% extract the non-zero terms
extract

% plot computed parameters
plot_reconstructed_parameters

```



## Applications

## Applications

Exponential analysis in physical phenomena:

- ▶ power system transient detection
- ▶ motor fault diagnosis
- ▶ drug clearance / glucose tolerance
- ▶ magnetic resonance / infrared spectroscopy
- ▶ vibration analysis
- ▶ seismic data analysis
- ▶ music signal processing
- ▶ corrosion rate / crack initiation
- ▶ odour recognition with electronic nose
- ▶ typed keystroke recognition
- ▶ liquid (explosive) identification
- ▶ ...



Figure: Transient detection and characterization

## Transients

## Transients

short lived high frequency signal:

- ▶ speech processing
- ▶ turbulent flow
- ▶ power lines
- ▶ ...

- ▶ model with  $\phi_i = 120\pi i$ ,

$$\sum_{i=1}^n \alpha_i \cos(120\pi x + \gamma_i) \mathbf{1}_{[A_i, Z_i[}$$

- ▶  $n = 3, \alpha_i = 1, \gamma_{1,3} = -\pi/2, \gamma_2 = 3\pi/4$
- ▶  $[A_1, Z_1[ = [0, 0.0308[$
- ▶  $[A_2, Z_2[ = [0.0308, 0.0625[$
- ▶  $[A_3, Z_3[ = [0.0625, 0.1058[$
- ▶  $M = 1200$
- ▶ uniformly distributed noise in  $[-0.05, 0.05]$

## Transients

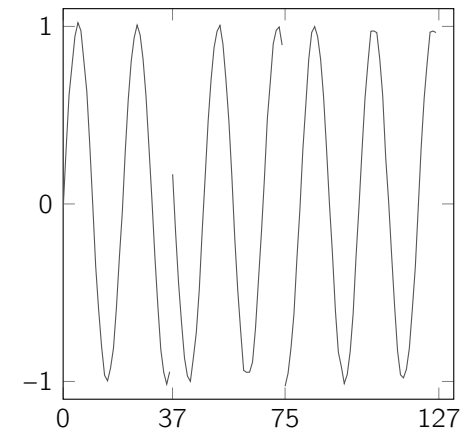


Figure: Given transient signal

## Transients



- ▶ at each instance: 2 exponential terms
- ▶ characteristics of terms change
- ▶ inspect rank of

$$H_4^{(1)} = \begin{pmatrix} f_1 & f_2 & f_3 & f_4 \\ f_2 & f_3 & f_4 & f_5 \\ f_3 & f_4 & f_5 & f_6 \\ f_4 & f_5 & f_6 & f_7 \end{pmatrix}$$

$$[A_1, Z_1] = [0/M, 37/M[,$$

$$[A_2, Z_2] = [37/M, 75/M[,$$

$$[A_3, Z_3] = [75/M, 127/M[$$

## Transients

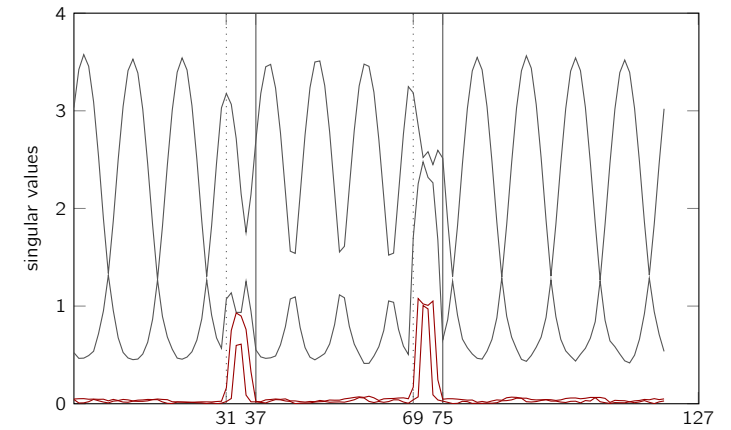


Figure: Numerical rank of  $H_4^{(r)}$  evolving over time  $x$

## Transients

## Audio signals



Figure: Reconstructing undersampled audio signals

## Audio signals

song containing 29 notes of 0.25 seconds each:

- ▶  $M = 44100$  (Hz)
- ▶ 11025 samples per note, 319725 in total
- ▶  $16.35 \leq \phi_i \leq 4978.03$ ,  $i = 1, \dots, 100$
- ▶ complex exponential model

## Audio signals

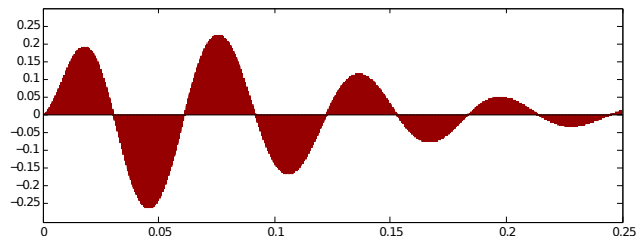


Figure: Sampled signal produced by 1 note

## Audio signals

compressive sensing (optimisation, probabilistic)

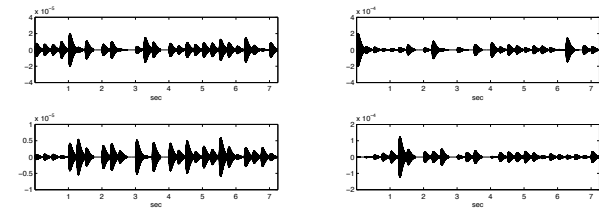


Figure: 4 runs with 1229 samples

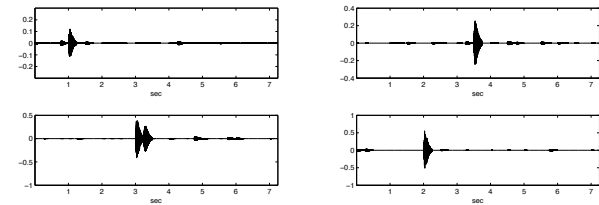


Figure: 4 runs with 456 samples

## Audio signals

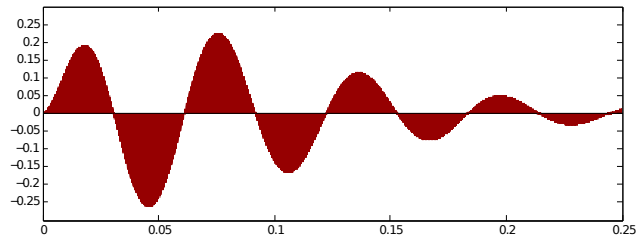


Figure: Full set of samples per note

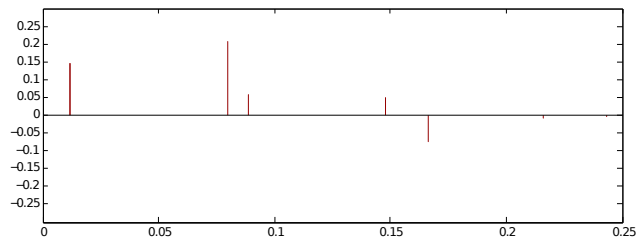


Figure: Sparse interpolation with 7 samples per note

## MCSA



Figure: Preventive diagnosis of a broken rotor bar

# MCSA

3-phase induction motors:

- ▶ consume 40 – 50% of all electricity in industrialized countries
- ▶ rotor made up metal bars
- ▶ stator current signal analysed
- ▶ broken bar(s) characterized by sideband frequencies
- ▶ difficult to diagnose under low or no load

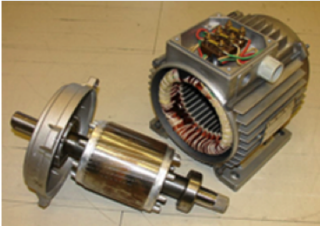


Figure: Stator and rotor

# MCSA

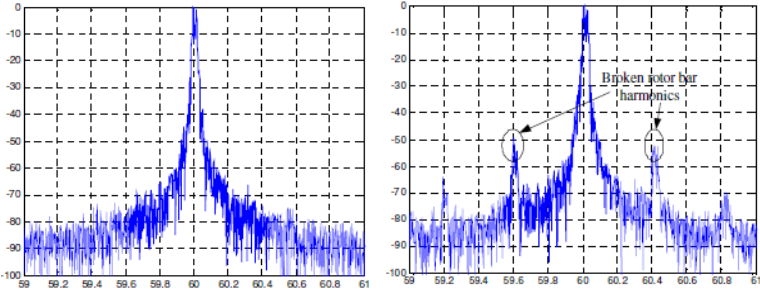


Figure: Stator current FFT spectra: healthy and with 1 broken bar

# MCSA

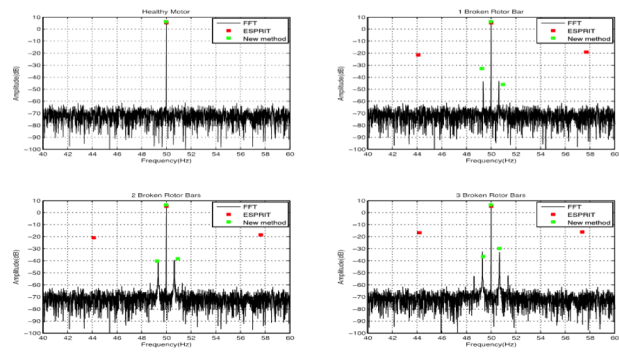


Figure: 10% load, 16dB noise,  $\nu = 400$

# Bio-electrical



Figure: Sparse EEG approximation

## Bio-electrical

Bio-electrical signals:

- ▶ electrical activity of cells and tissues
- ▶ clinical studies of health status
- ▶ ECG, EEG, EMG, EOG, . . .
- ▶ sparse model ( $n = 8$ ) is approximate

## Bio-electrical

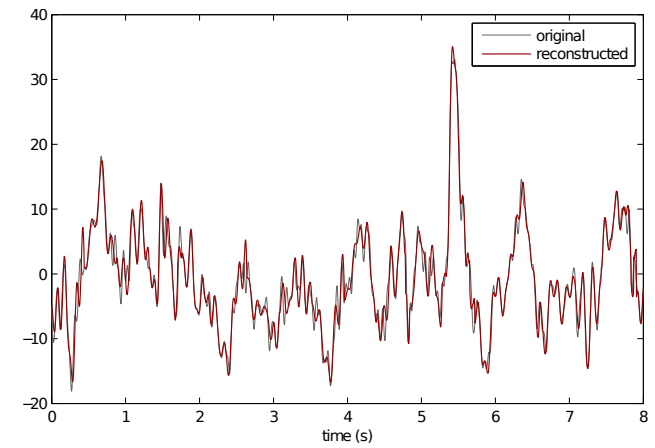


Figure: Reconstruction of 8 second [1 – 20] Hz bandpass filtered EEG

## Bio-electrical



Figure: Sparse EOG approximation

## Bio-electrical

### Polysomnogram:

- ▶ 12 channels
- ▶ 22 wire attachments to patient
- ▶ heart rate, leg measurement, airflow (chest, abdomen), chin muscle, EEG, EOG, . . .



Sparse Interpolation

- Motivation
- Basics: exponential
- Basics: polynomial
- Approximation theory
- Applications**
- References

## Bio-electrical

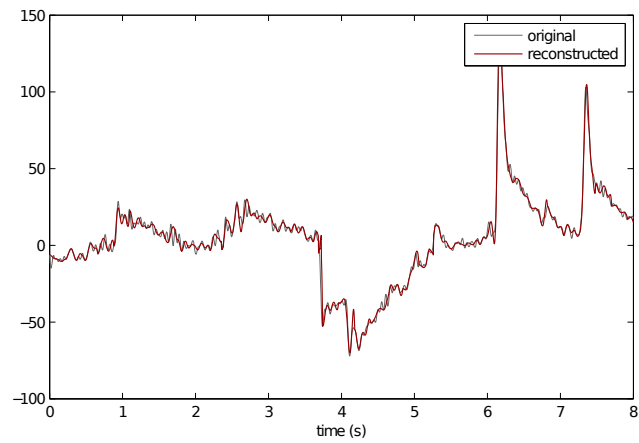


Figure: Reconstruction of 8 second EOG (CC = 99.2%)

Sparse Interpolation

- Motivation
- Basics: exponential
- Basics: polynomial
- Approximation theory
- Applications**
- References

## Spectroscopy

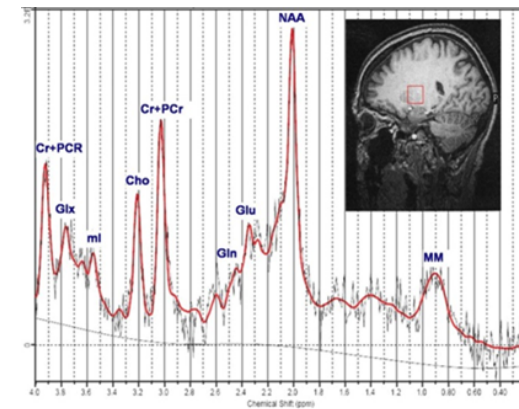


Figure: Spectral analysis of FID

## Spectroscopy

Magnetic resonance spectroscopy:

- ▶ physical and chemical properties of molecules
- ▶ a.o. concentration of metabolites in the brain
- ▶ frequencies clustered → high frequency resolution
- ▶ free induction decay → time constraint
- ▶ Fourier methods need additional tools

## Spectroscopy

$$\phi(x) = 5 \times 10^{-2} + 2e^{(-0.97+i79.94\pi)x} + 4e^{(-1+i80\pi)x} + 8e^{-1.1x} + \varepsilon(x)$$

$\|\varepsilon(x)\|_{\infty} = 10^{-3}$ ,      circular Gaussian noise

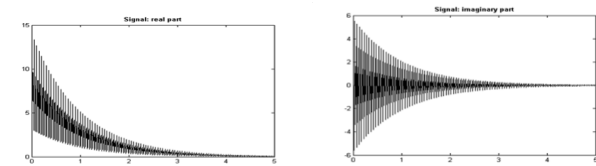


Figure: The real (left) and imaginary (right) part of  $\phi(x)$

## Spectroscopy

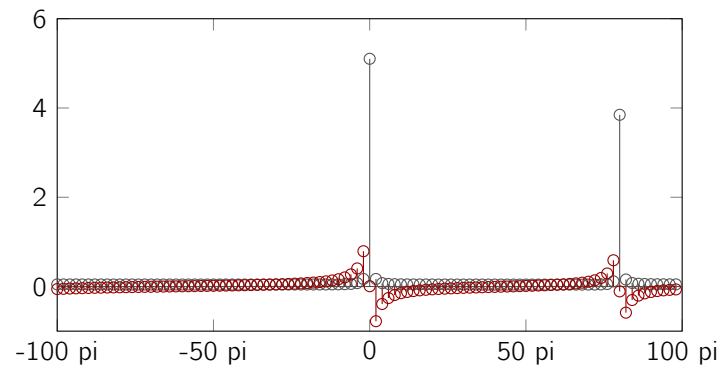


Figure: Real (black) and imaginary (red) parts of FFT

## Spectroscopy

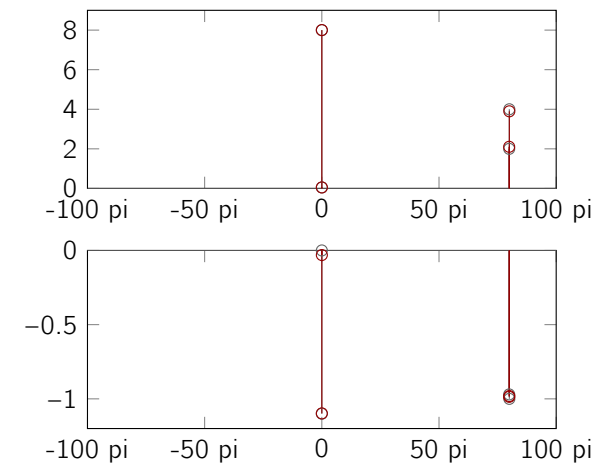


Figure: Amplitudes (top) and damping factors (bottom) of  $\phi(x)$

## References

## References

- M. Ben-Or and P. Tiwari. A deterministic algorithm for sparse multivariate polynomial interpolation. In *STOC '88: Proceedings of the twentieth annual ACM symposium on Theory of computing*, pages 301–309, New York, NY, USA, 1988. ACM. <http://dx.doi.org/10.1145/62212.62241>.
- M. de Montessus de Ballore. Sur les fractions continues algébriques. *Rend. Circ. Mat. Palermo*, 19:185–257, 1905. <http://dx.doi.org/10.1007/BF03014011>.
- R. de Prony. Essai expérimental et analytique sur les lois de la dilatabilité des fluides élastiques et sur celles de la force expansive de la vapeur de l'eau et de la vapeur de l'alkool, à différentes températures. *J. Ec. Poly.*, 1:24–76, 1795.
- M. Giesbrecht, G. Labahn, and W. Lee. Symbolic-numeric sparse interpolation of multivariate polynomials. In *ISSAC'06*, 2006. <http://dx.doi.org/10.1145/1145768.1145792>. 9–12 July.
- P. Henrici. *Applied and computational complex analysis I*. John Wiley & Sons, New York, 1974.
- Y. Hua and T. K. Sarkar. Matrix pencil method for estimating parameters of exponentially damped/undamped sinusoids in noise. *IEEE Trans. Acoust. Speech Signal Process.*, 38:814–824, 1990. <http://dx.doi.org/10.1109/29.56027>.
- E. Kaltofen and W.-s. Lee. Early termination in sparse interpolation algorithms. *J. Symbolic Comput.*, 36(3-4):365–400, 2003. [http://dx.doi.org/10.1016/S0747-7171\(03\)00088-9](http://dx.doi.org/10.1016/S0747-7171(03)00088-9). International Symposium on Symbolic and Algebraic Computation (ISSAC'2002) (Lille).
- J. L. Massey. Shift-register synthesis and BCH decoding. *IEEE Trans. Inform. Theory*, 15(1):122–127, 1969. <http://dx.doi.org/10.1109/TIT.1969.1054260>.
- J. Nuttall. The convergence of Padé approximants of meromorphic functions. *J. Math. Anal. Appl.*, 31:147–153, 1970. [http://dx.doi.org/10.1016/0022-247X\(70\)90126-5](http://dx.doi.org/10.1016/0022-247X(70)90126-5).
- H. Padé. *Sur la représentation approchée d'une fonction par des fractions rationnelles*. PhD thesis, Faculté des sciences de Paris, 1892.
- C. Pommerenke. Padé approximants and convergence in capacity. *J. Math. Anal. Appl.*, 41:775–780, 1973. [http://dx.doi.org/10.1016/0022-247X\(73\)90248-5](http://dx.doi.org/10.1016/0022-247X(73)90248-5). 77/77